TOXICOLOGICAL SCIENCES **103(1)**, 97–107 (2008)
doi:10.1093/toxsci/kfn031
Advance Access publication February 14, 2008

3,4-Dichloropropionanilide (DCPA) Inhibits T-Cell Activation by Altering the Intracellular Calcium Concentration following Store Depletion

Tricia L. Lewis,*,† Kathleen M. Brundage,*,† Rodney A. Brundage,‡,[1] and John B. Barnett*,†,[2]

*Department of Microbiology, Immunology and Cell Biology; †Center for Immunopathology and Microbial Pathogenesis, West Virginia University School of Medicine, Morgantown, West Viginia 26506; and ‡National Institute for Occupational Safety and Health, Centers for Disease Control and Prevention, U.S. Department of Health and Human Services, Morgantown, West Viginia 26506

Received February 8, 2008; accepted February 10, 2008

Stimulation of T cells through the T-cell receptor results in the activation of a series of signaling pathways that leads to the secretion of interleukin (IL)-2 and cell proliferation. Influx of calcium (Ca^{2+}) from the extracellular environment, following internal Ca^{2+} store depletion, provides the elevated and sustained intracellular calcium concentration ($[Ca^{2+}]_i$) critical for optimal T-cell activation. Our laboratory has documented that exposure to the herbicide 3,4-dichloropropionanilide (DCPA) inhibits intracellular signaling events that have one or more Ca^{2+} dependent steps. Herein we report that DCPA attenuates the normal elevated and sustained $[Ca^{2+}]_i$ that follows internal store depletion in the human leukemic Jurkat T cell line and primary mouse T cells. DCPA did not alter the depletion of internal Ca^{2+} stores when stimulated by anti-CD3 or thapsigargin demonstrating that early inositol 1,4,5-triphosphate–mediated signaling and depletion of Ca^{2+} stores were unaffected. 2-Aminoethyldiphenol borate (2-APB) is known to alter the store-operated Ca^{2+} (SOC) influx that follows Ca^{2+} store depletion. Exposure of Jurkat cells to either DCPA or 50μM 2-APB attenuated the increase in $[Ca^{2+}]_i$ following thapsigargin or anti-CD3 induced store depletion in a similar manner. At low concentrations, 2-APB enhances SOC influx but this enhancement is abrogated in the presence of DCPA. This alteration in $[Ca^{2+}]_i$, when exposed to DCPA, significantly reduces nuclear levels of nuclear factor of activated T cells (NFAT) and IL-2 secretion. The plasma membrane polarization profile is not altered by DCPA exposure. Taken together, these data indicate that DCPA inhibits T-cell activation by altering Ca^{2+} homeostasis following store depletion.

Key Words: **T cells; signal transduction; calcium; 3,4-dichloropropionanilide; propanil.**

The herbicide 3,4-dichloropropionanilide (DCPA), commonly referred to as propanil, is applied predominantly on rice fields for control against several broadleaf and grassy weeds. Annual use of DCPA is estimated to be 7 million pounds per year. The broad application and heavy use of this herbicide underscores the importance of investigating its immunotoxic effects.

In vivo administration of DCPA to mice results in decreased *ex vivo* cytokine production by macrophages (interleukin [IL]-1β, IL-6, and tumor necrosis factor [TNF]-α) and T cells (IL-2 and interferon-γ) (Barnett *et al.*, 1992; Zhao *et al.*, 1998). Lipopolysaccharide-stimulated macrophages demonstrated a decrease in intracellular calcium concentration ($[Ca^{2+}]_i$) after exposure to DCPA (Xie *et al.*, 1997). Murine lymphoma T cell (EL-4) and human Jurkat T cell lines exposed to DCPA show decreased IL-2 production and IL-2 mRNA levels (Brundage *et al.*, 2004; Zhao *et al.*, 1999). In addition, Jurkat cells exposed to DCPA demonstrate decreased DNA binding ability of the transcription factor, activating protein-1 (AP-1), and decreased c-jun protein (Brundage *et al.*, 2004).

Activation of T cells is initiated through recognition of a peptide presented on the surface of an antigen presenting cell, along with costimulatory interactions, which triggers a series of events including phosphorylation of the TCR complex and recruitment of kinases and adapter proteins to the plasma membrane (PM). Subsequent activation of phospholipase-$C\gamma_1$ results in the hydrolysis of phosphatidylinositol 4,5-bisphosphate and the production of two second messengers, diacylglycerol (DAG) and inositol 1,4,5-triphosphate (IP_3) (Feske *et al.*, 2003; Panyi *et al.*, 2004). DAG remains in the PM and activates proteins such as protein kinase C. IP_3 is released from the PM and interacts with the IP_3-receptor on the surface of the endoplasmic reticulum (ER) resulting in the release of Ca^{2+} from the ER. Depletion of ER Ca^{2+} stores activates store-operated Ca^{2+} (SOC) channels located on the PM allowing for the influx of Ca^{2+} from the extracellular environment. This results in an increased and sustained $[Ca^{2+}]_i$ and activation, via calmodulin, of calcineurin, which leads to the dephosphorylation of nuclear factor of activated T cells (NFAT) and its translocation into the nucleus. Once in the nucleus NFAT acts as a transcription factor for the production of key cytokines (Feske *et al.*, 2003). Ca^{2+} also plays a role in the activation of the transcription factors nuclear factor kappa B (NF-κB), and AP-1 (Lewis, 2001;

[1] Present address: Department of Microbiology, Immunology and Cell Biology, West Virginia University School of Medicine, Morgantown, WV 26506.

[2] To whom correspondence should be addressed at Department of Microbiology, Immunology and Cell Biology, PO Box 9177, West Virginia University, Morgantown, WV 26506-9177. Fax: (304) 293-7823. E-mail: jbarnett@hsc.wvu.edu.

Quintana *et al*., 2005). Cooperative binding of these three transcription factors is required for optimal transcription and production of IL-2, an essential early cytokine required for T-cell proliferation and differentiation (Garrity *et al*., 1994).

The importance of calcium as a second messenger in T-cell activation has been well established (Feske, 2007; Lewis, 2001; Quintana *et al*., 2005). Two coupled mechanisms exist to provide the necessary $[Ca^{2+}]_i$ required for optimal T-cell activation. The first mechanism involves an initial increase in $[Ca^{2+}]_i$ through the IP_3-mediated depletion of ER Ca^{2+} stores. This transient increase is necessary but not sufficient for optimal T-cell activation (Feske *et al*., 2006). Emptying of the ER Ca^{2+} stores is coupled to the activation of Ca^{2+}-release activated Ca^{2+} (CRAC) channels on the PM. Upon ER store depletion STIM-1 (stromal interaction molecule-1) redistributes into puncta on the ER and accumulates close to the PM (Wu *et al*., 2006; Xu *et al*., 2006; Zhang *et al*., 2005). Orai1 (also known as CRACM1) has recently been described as an essential pore subunit of the CRAC channel (Prakriya *et al*., 2006; Vig *et al*., 2006). During T-cell activation, aggregation of STIM-1 on the ER induces clustering of Orai1 on the PM resulting in an influx of Ca^{2+} through the CRAC channel (Xu *et al*., 2006). This increase in $[Ca^{2+}]_i$ through the CRAC channels is essential for the activation of transcription factors necessary for cytokine production. Defects in the CRAC channel have been reported in patients with severe combined immunodeficiency syndrome, underscoring the importance of Ca^{2+} influx through CRAC channels in T-cell activation (Feske *et al*., 2000, 2001, 2005).

Due to the importance of Ca^{2+} homeostasis in T-cell activation and function, we investigated the effect of DCPA on $[Ca^{2+}]_i$ in T cells, using primary mouse T cells and the Jurkat human T cell line. The human Jurkat T cell line has been used as a model for human T-cell signaling for over two decades (Abraham and Weiss, 2004). In this report, we define more clearly the mechanism of the effect of DCPA on T cells. Our experiments indicate that DCPA inhibits T-cell activation by attenuating increases in $[Ca^{2+}]_i$ following the depletion of internal Ca^{2+} stores.

MATERIALS AND METHODS

Cell lines. Experiments were performed using the human T-cell leukemia cell line, Jurkat clone E6-1, obtained from the American Tissue Culture Collection (Manassas, VA). Jurkat cells were maintained in complete Roswell Park Memorial Institute (RPMI) 1640 media (Mediatech, Inc., Herndon, VA) supplemented with 10% heat inactivated fetal bovine serum (vol/vol) (FBS) (Hyclone, Inc. Logan, UT), 100 units/ml penicillin (Bio Whittaker, Walkersville, MD), 100 μg/ml streptomycin (Bio Whittaker), 20mM glutamine (Bio Whittaker), and 50μM 2-mercaptoethanol (Sigma, St Louis, MO). The cultures were kept at 37°C in 5% CO_2. During the course of the experiments, no significant change in cell viability was observed in cells treated with vehicle control or 50-200 μM DCPA.

Mice. Female BALB/c mice (8–10 weeks old) were purchased from Charles River Labs (Wilmington DE). Mice were housed in the vivarium at West Virginia University Health Sciences Center under the care of a full time veterinarian and professional staff. They were given access to food and water *ad libitum* and allowed to acclimate to the facility for at least 1 week prior to use. Experiments were conducted in accordance with all federal and institutional guidelines for animal use and were approved by the West Virginia University Institutional Animal Care and Use Committee.

Isolation of mouse T cells. Spleens from BALB/c mice were removed aseptically, pooled and made into a single cell suspension. Red blood cells were lysed using Tris–NH_4Cl and resuspended in sorting buffer (phosphate buffered saline [PBS], 0.5% bovine serum albumin [BSA], and 2mM disodium ethylenediamine tetraacetate [EDTA]) at 2.5×10^5 cells/ml. An enriched (> 90% by flow cytometry) population of T cells was isolated through negative selection using the Pan T cell isolation kit (Miltenyi Biotech, Auburn, CA). Briefly, spleen cells were incubated at 4°C for 10 min with a cocktail of biotin-conjugated monoclonal antibodies specific for CD14, CD16, CD19, CD36, CD56, CD123, and Glycophorin A, as described in the manufacturer's protocol (Miltenyi Biotec). Next, monoclonal anti-biotin antibody-conjugated magnetic microbeads were added to the sample and incubated for 15 min at 4°C. Cells were washed with sorting buffer and resuspended at 1×10^8 cells in 500 μl of cold buffer. Cells were then loaded onto autoMACS columns (Miltenyi Biotec) and purified T cells were collected through a negative selection process. Purified T cells were stimulated using anti-CD3 (BD Biosciences, San Diego, CA) and goat anti-Armenian hamster antibody (Jackson ImmunoResearch, West Grove PA) to crosslink the anti-CD3 as previously described (Kubo *et al*., 1989).

Fluorescence measurement of $[Ca^{2+}]_i$. Jurkat cells or splenic mouse T cells were loaded with the calcium-indicator dye fluo-3 AM (Invitrogen, Carlsbad, CA) as previously described (Grynkiewicz *et al*., 1985). Briefly, cells were harvested and resuspended to a concentration of 5×10^6 cells/ml and incubated for 30 min (37°C in 5% CO_2) in complete RPMI 1640 media (1.5% FBS, vol/vol) containing 0.1μM fluo-3 AM in the presence of 0.02% pluronic F-127 (Invitrogen) and 2.5mM probenecid (Sigma). Cells were then washed twice in Ca^{2+} and Mg^{2+}-free Hanks Balanced Salt Solution (HBSS) (Mediatech, Inc.) containing 10mM N-(2-hydroxyethyl)-piperazine-N'-2-ethanesulfonic acid (HEPES), pH 7.4, 2% FBS and 2.5mM probenecid, resuspended to a concentration of 1×10^6 cells/ml and incubated 30 min at room temperature. Because the addition of 2% FBS is essential for cell viability the media contains a nominal concentration of Ca^{2+} (2.5μM). Samples were kept at room temperature and protected from light until ready for analysis. 2×10^6 cells were placed in a quartz cuvette and the fluorescence was measured using a PTI QM-2000-4 spectrofluorometer (Photon Technology International [PTI], Birmingham, NJ) with constant stirring. The fluorescence of the fluo-3 dye was measured with excitation at 490 nm and emission at 525 nm. Stock solutions of DCPA (ChemServices, West Chester, PA) and 2-aminoethyldiphenol borate (2-APB) (CalBioChem, San Diego, CA) were diluted in absolute ethanol (AAPER Alcohol and Chemical Company, Shelbyville, KY). Vehicle samples were treated with an equivalent concentration (0.1% vol/vol) of ethanol. The fluorescence was measured and digitized at 1 Hz using the software program FeliX 1.42b (PTI). Experiments using Jurkat cells were treated as follows: approximately 45 s after starting data collection, 2.0 μl of DCPA, 2-APB or vehicle was added to the cuvette, and stimulated immediately with mouse anti-human CD3 antibody at a final concentration of 5.0 μg/ml (UCHT1) (BD Biosciences, San Diego, CA). Experiments using splenic mouse T cells were treated with DCPA or vehicle control and stimulated immediately with anti-CD3 (BD Bioscience) and goat anti-Armenian hamster antibody (Jackson ImmunoResearch, West Grove PA) to crosslink the anti-CD3 as previously described (Kubo *et al*. 1989). When the fluorescence returned to background levels, $CaCl_2$ (Fluka, Switzerland) was added (final concentration 2.5mM) to the media to provide an external source of Ca^{2+}. Addition of ionomycin (final concentration 200μM) (Sigma) provided evidence that the cells were loaded evenly and that the dye remained in the cytosol. Cell membranes were lysed with 0.1%, vol/vol Triton X-100 (Fisher Scientific, Hampton, NH) to measure the maximum fluorescence (F_{max}) parameter for calculation of $[Ca^{2+}]_i$, to monitor compartmentalization of the dye and ensure the amount of dye was not a limiting factor. Ethylene glycol-bis(β-aminoethyl ether)-N,N,N′,N′-tetraacetic acid tetrasodium salt (EGTA) (Sigma) was added to a final concentration of 50mM (pH 7.5) to lower the free Ca^{2+} to a nominally Ca^{2+}-free level (F_{min}).

Fluorescence values were converted to $[Ca^{2+}]_i$ using the following equation:

$$\text{free}[Ca^{2+}]_i = K_D[(F - F_{min})/(F_{max} - F)],$$

where K_D (360nM) is the dissociation constant of the Fluo-3/Ca^{2+} complex, F is the measured fluorescence intensity, F_{min} is the minimum fluorescence at very low $[Ca^{2+}]_i$ (fluorescence after the addition of 50mM EGTA) and F_{max} is the fluorescence measured at high $[Ca^{2+}]_i$ (fluorescence after the addition of Triton X-100) (Grynkiewicz *et al*., 1985). The background fluorescence obtained from unloaded cells over a 3-min time period was subtracted from all data points before $[Ca^{2+}]_i$ was calculated.

Measurement of IL-2 production. Jurkat cells were cultured in complete RPMI 1640 media or RPMI 1640 media without Ca^{2+} at 5×10^5 cells/well in 48-well plates (Costar, Corning, NY) coated with mouse anti-human CD3 antibody (10 μg/ml) (BD Bio Sciences, San Diego, CA). Cells were treated with 25, 50, 100, 125, or 200μM DCPA, or vehicle control. DCPA solutions were diluted in absolute ethanol and vehicle control samples were given an equivalent amount of absolute ethanol (0.1% vol/vol). Cells were also simultaneously stimulated with anti-CD28 antibody (2 μg/ml) (BD PharMingen, San Diego, CA). Cells were incubated at 37°C in 5% CO_2 for 48 h after which supernatants were collected and placed at −20°C. IL-2 production was determined using the sandwich enzyme-linked immunosorbent assay (ELISA) method and following the manufacturer's protocol (BD PharMingen). All cultures and ELISA analyses were performed in triplicate and the experiment was repeated three times.

Nuclear extracts. Jurkat cells were cultured to 1×10^6 cells/ml in complete RPMI 1640 and stimulated with 10 ng/ml phorbol myristate acetate (PMA) (Sigma-Aldrich) and 1 μg/ml A23187 (Sigma-Aldrich). Cells were treated with 0.1% vol/vol ethanol (vehicle control), 100μM DCPA, or received no treatment. After a 1, 2, 4, and 6 h exposure, cells were harvested and centrifuged at 330 × g for 8 min at 4°C. Nuclear extracts were prepared as previously described (Schreiber *et al*., 1989). Briefly, cells were resuspended in 1 ml of PBS, pelleted, resuspended in cold buffer A (10mM HEPES pH 7.9, 10mM KCL, 0.1mM EDTA, 0.1mM EGTA, 1mM DTT [dithiothreitol], and 0.5mM PMSF [phenylmethanesulfonyl fluoride]) and incubated on ice for 15 min. After incubation, 25 μl of a 10% solution of Nonidet NP-40 was added, vortexed and centrifuged for 30 s at 14,000 × g. Supernatants, containing the cytoplasmic fraction of the cells, were frozen at −70°C. The nuclear pellet was resuspended in cold buffer C (20mM HEPES pH 7.9, 0.4M NaCl, 1mM EDTA, 1mM EGTA, 1mM DTT, and 1mM PMSF) and incubated on ice for 15 min with vortexing every 5 min. Samples were centrifuged for 5 min at 14,000 × g and the supernatants containing the nuclear fraction were stored at −70°C. The protein concentrations of the nuclear extracts were determined using Coomassie plus protein assay reagent kit following the manufacturer's protocol (Pierce, Rockford, IL).

Western blots. A 30-μg aliquot of each nuclear extract was boiled for 5 min to denature the proteins and electrophoresed through an 8% Tris polyacrylamide gel with a 4% stacking gel at 25 mA for 18 h. Proteins were transferred onto Hybond-P membranes (Amersham Pharmacia, Piscataway, NJ) at 0.1 A for 20 h. Blots were washed in TBS for 5 min at room temperature, blocked for 1 h in Tris Buffered Saline (TBS) + 0.1% Tween 20 (TBS/T) plus 5% dry milk at room temperature and then washed three times in TBS/T. Blots were incubated overnight at 4°C with primary antibodies specific for total NFATc2 (Santa Cruz Santa Cruz, CA) or β-actin (Santa Cruz) in TBS/T plus 5% BSA. The next day, blots were washed three times in TBS/T, incubated for 1 h at room temperature with anti-biotin (Cell Signaling Technology, Inc., Danvers, MA) and either a goat anti-mouse IgG-horseradish peroxidase (HRP) (Santa Cruz) or a rabbit anti-goat IgG-HRP (Sigma-Aldrich). Finally, the blots were washed three times in TBS/T and developed using Phototope-HRP detection kit for Western blots (Cell Signaling Technology, Inc.) and bands were visualized on X-Ray film (BioMax MR, Eastman Kodak Company). Densitometric analysis was performed using Optimus software (Media Cybernetics, Silver Spring, MD) and nuclear NFAT protein levels were normalized to actin protein levels for each sample.

Measurement of membrane potential. The membrane potential of Jurkat cells was measured using the membrane potential-sensitive $DiBAC_4(3)$ dye (Invitrogen). This bis-oxonol dye produces an excitation maximum at approximately 490 nm. As the cell depolarizes increasing amounts of dye enters the cell where it binds to intracellular proteins or membranes and exhibits enhanced fluorescence. Conversely, hyperpolarization is indicated by a decrease in fluorescence. $DiBAC_4(3)$ is excluded from mitochondria because of its overall negative charge, allowing measurement of the PM potential (Wolff *et al*., 2003). Membrane potential experiments were carried out in a time course similar to the fluo-3 experiments. Briefly, 1×10^6 cells/ml of Jurkat cells were suspended in Ca^{2+} and Mg^{2+}-free HBSS (Mediatech, Inc.) containing 10mM HEPES, pH 7.4 and 2% FBS containing 20nM $DiBAC_4(3)$. Samples were kept at room temperature and protected from light until ready for analysis. A 1.0 ml (1×10^6 cells) aliquot of loaded cells was placed in a tube and the fluorescence was measured using a FACSCalibur flow cytometer (Becton Dickson, Franklin Lakes, NJ). Each recorded time point consisted of 10,000 cells. At $t = 0$ a background fluorescence was recorded after which DCPA, or vehicle control was added, followed immediately by anti-CD3 antibody at a final concentration of 5.0 μg/ml (BD Biosciences). Fluorescence measurements were recorded immediately following treatment and anti-CD3 addition ($t = 1$ min) and again at $t = 3$ min and $t = 5$ min. External Ca^{2+}, in the form of $CaCl_2$, (Fluka, Switzerland) was subsequently added (final concentration 2.5mM) to the cells to provide an external source of Ca^{2+}. Fluorescence measurements were collected at three time points following addition of external Ca^{2+} ($t = 5.5$, 6.5, and 9.5 min). Addition of 40 μl of KCl (final concentration 100mM) completely depolarized the cell and fluorescence values were recorded at $t = 10$, 12, and 14 min. Background fluorescence of unloaded cells was subtracted from all data points before the net change in fluorescence was calculated. The fluorescence was represented as the net change in the fluorescence signal as a percent of the initial background fluorescence (F_0) of the T cells at rest as described by $\Delta F/F_0 = (F_t - F_0) \times 100/F_0$ (where F_t is the fluorescence at each time point) (Wolff *et al*., 2003).

Statistical analysis. All data were analyzed using MS Excel 2003 (Redmond, WA) and Sigma Stat 3.1 (Port Richmond, CA). The area under the curve (AUC) is an indirect measurement of the increase of $[Ca^{2+}]_i$ over a selected time period. The AUC includes all data points from the time the external Ca^{2+} was added until the $[Ca^{2+}]_i$ reached a plateau and was calculated using Sigma Stat 3.1. The peak $[Ca^{2+}]_i$ was calculated by determining the highest $[Ca^{2+}]_i$ between addition of $CaCl_2$ and addition of ionomycin. ANOVA with a Student-Newman-Keuls post hoc test was used to analyze the AUC and peak $[Ca^{2+}]_i$ in DCPA-treated cells (Fig 1 and 3). ANOVA was used to determine statistical significance in IL-2 production. A t-test was used to determine statistical significance for membrane potential experiments and fluorescence experiments in Fig 2 and 3. An alpha value of < 0.05 was considered significant.

RESULTS

Effect of DCPA on $[Ca^{2+}]_i$ in anti-CD3 Stimulated Jurkat Cells

T-cell activation and proliferation requires a cascade of signaling events mediated by two Ca^{2+} sensitive mechanisms. The first involves the IP_3-mediated depletion of Ca^{2+} stores in the ER and is coupled to the second mechanism, the activation of CRAC channels and the influx of Ca^{2+}. Stimulation of Jurkat T cells with anti-CD3 results in activation of membrane proximal responses that includes release of IP_3, binding to the IP_3 receptor on the ER, and release of ER Ca^{2+} stores enabling activation of CRAC channels. To determine the effect of DCPA on early $[Ca^{2+}]_i$ signaling events Jurkat cells, loaded with fluo-3 in a nominally Ca^{2+}-free (2.5μM) HBSS solution, were treated with 25, 50, 100, 200μM DCPA or vehicle (ethanol) control and stimulated with anti-CD3. At this time, there is no data available

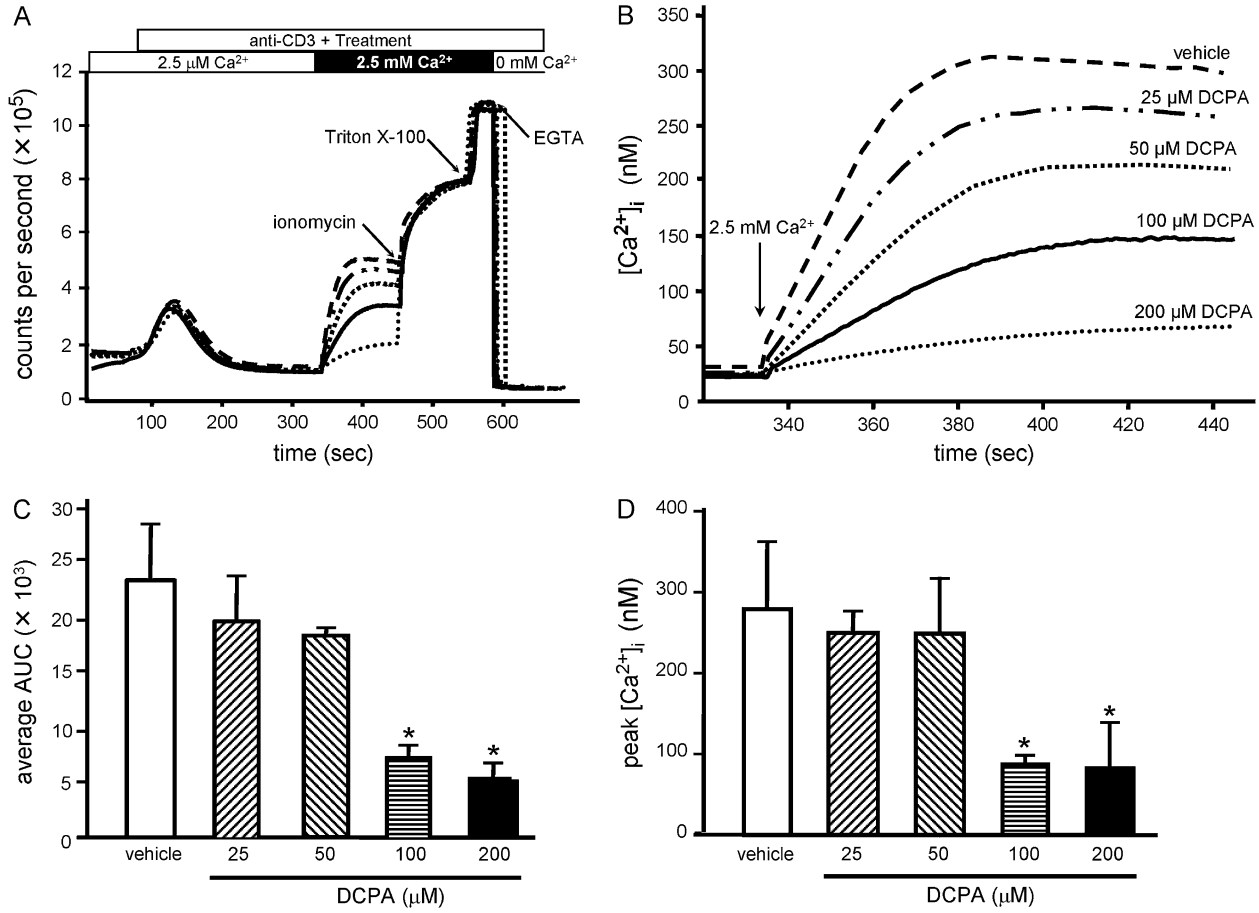

FIG. 1. The concentration dependent effect of DCPA on $[Ca^{2+}]_i$ in anti-CD3 stimulated Jurkat cells. Jurkat cells were loaded with fluo-3 in a nominally Ca^{2+}-free solution. At 50 s, anti-CD3 was added simultaneously with 25, 50, 100, or 200μM DCPA or vehicle control and changes in $(Ca^{2+})_i$ were recorded with a spectrofluorometer. At 335 s, the external $[Ca^{2+}]$ concentration was increased to 2.5mM with $CaCl_2$. Starting at 442 s, ionomycin, Triton X-100 and EGTA were sequentially added to the cell media at the times indicated. (A) A representative experiment of the complete fluorescence curve in the absence and presence of DCPA at increasing concentrations. (B) Conversion of the fluorescence intensity from part (A) to a $[Ca^{2+}]_i$ for $t = 320$–442 s. (C) Statistical analysis of the AUC for DCPA and vehicle control from three separate experiments. (D) Statistical analysis of the peak $[Ca^{2+}]_i$ for DCPA and vehicle control from three separate experiments. Error bars reflect the ± SD and asterisks (*) indicates statistically significant results, $p < 0.05$. Statistical analysis was performed using an ANOVA with a Student-Newman-Keuls post hoc test.

that correlates *in vitro* exposure concentrations with measured *in vivo* tissue concentrations in mice exposed to DCPA. The range of DCPA was selected based on published concentrations that correspond to immune effects (Brundage *et al*. 2004; Corsini *et al*. 2007). We determined that DCPA and ethanol, hereafter referred to as the vehicle, did not interfere with the fluorescence of the fluo-3 dye (data not shown). There was no significant difference between cells stimulated with anti-CD3 or cells that were exposed to vehicle and stimulated with anti-CD3 (data not shown). As shown in Figure 1, addition of DCPA or vehicle followed by stimulation with anti-CD3, in a nominally Ca^{2+}-free environment, resulted in an equivalent small, transient increase in fluorescence (t=50-335 s). This increase in the $[Ca^{2+}]_i$ represents the depletion of IP_3-sensitive Ca^{2+} stores and its subsequent removal out of the cell by activated Ca^{2+}-adenosine triphosphatases (ATPases) or its sequestration within the cell. DCPA and vehicle treated cells exhibited similar changes in $[Ca^{2+}]_i$ indicating that DCPA does not affect the early IP_3-mediated signaling pathway or the depletion of internal Ca^{2+} stores.

In T cells, optimal activation of several transcription factors requires a sustained and elevated $[Ca^{2+}]_i$ that is maintained by Ca^{2+} influx through CRAC channels following internal Ca^{2+} store depletion. To determine if DCPA alters $[Ca^{2+}]_i$ following store depletion we added Ca^{2+} to the media following anti-CD3 induced store depletion (Fig. 1A t=337-440 s). Figure 1B is an expanded view of the change in $[Ca^{2+}]_i$ following store depletion (t=337-440 s from Fig. 1A) represented as a $[Ca^{2+}]_i$. The $[Ca^{2+}]_i$ was calculated, using the fluorescence from Figure 1A, based on the equations described in Materials and Methods. A decrease in the $[Ca^{2+}]_i$, following store depletion was observed in Jurkat cells exposed to all four DCPA concentrations, when compared with the vehicle control

(Figs. 1A and 1B). Cells were further treated with ionomycin and Triton X-100 to monitor compartmentalization and ensure that the amount of available dye was not a limiting factor. In addition, Triton X-100 and EGTA provided maximum and minimum fluorescence values, respectively, to calculate the $[Ca^{2+}]_{i.}$ (see "Material and Methods"). Similar fluorescent levels after addition of ionomycin, Triton X-100 and EGTA were seen independent of treatment (Fig. 1A).

To further quantify the attenuation of the $[Ca^{2+}]_i$ following store depletion the AUC, peak $[Ca^{2+}]_{i,}$ and time to peak, were calculated. The AUC was calculated for each sample to determine the relative amount of free Ca^{2+} in the cytosol over a 103-s time period (t = 337–440 s). The AUC and peak $[Ca^{2+}]_i$ data for cells exposed to increasing concentrations of DCPA and stimulated with anti-CD3 are shown in Figures 1C and 1D. Exposure of cells to 200μM DCPA resulted in a significant decrease (79%) in the AUC and the peak $[Ca^{2+}]_i$ (78%). A 56% decrease in the AUC and a 52% decrease in the peak $[Ca^{2+}]_i$ was observed in cells treated with 100μM. Cells treated with 25 and 50μM DCPA also resulted in decreases in AUC and peak $[Ca^{2+}]_i$. In addition, the time to reach peak $[Ca^{2+}]_{i,}$ following addition of external Ca^{2+}, increased with increasing concentration of DCPA exposure. Vehicle control cells reached a peak $[Ca^{2+}]_i$ after approximately 65 s. Treatment of cells with 25, 50, 100, and 200μM DCPA resulted in a peak $[Ca^{2+}]_i$ at approximately 75, 81, 93, and 108 s, respectively. Using ANOVA, with a Student-Neuman-Keuls post hoc test, reveals a concentration-dependent effect in cells treated with increasing concentrations of DCPA. Increasing treatment of cells from 100 μM to 200 μM DCPA did not significantly decrease $[Ca^{2+}]_i$ so 100μM was used for all other experiments. Taken together, these results demonstrate that exposure to DCPA decreases $[Ca^{2+}]_i$ following anti-CD3 induced store depletion in a concentration dependent manner.

The Effect of DCPA on Thapsigargin Stimulated Jurkat Cells

To determine if exposure to DCPA affected the early IP_3-induced signaling pathway, the SERCA pump inhibitor thapsigargin was used. Thapsigargin depletes ER Ca^{2+} stores and prevents refilling, thereby activating Ca^{2+} influx through CRAC channels independent of IP_3 production (Bergling *et al.*, 1998). The addition of 100μM DCPA or vehicle control followed by 2μM thapsigargin resulted in an equivalent small, transient increase in fluorescence, similar to that observed with anti-CD3 stimulation (Fig. 2A). However, the normal increase in $[Ca^{2+}]_i$, following internal Ca^{2+} store depletion, is significantly decreased in DCPA-treated cells, compared with the vehicle control cells (Figs. 2A and 2B). Cells treated with thapsigargin and exposed to 100μM DCPA exhibited a significant decrease in the AUC and peak $[Ca^{2+}]_i$ similar to that observed with anti-CD3 stimulation (Figs. 2C and 2D). During a 70-s time period (t = 360–430 s) DCPA-exposed cells exhibited an approximately 50% decrease in the AUC and an

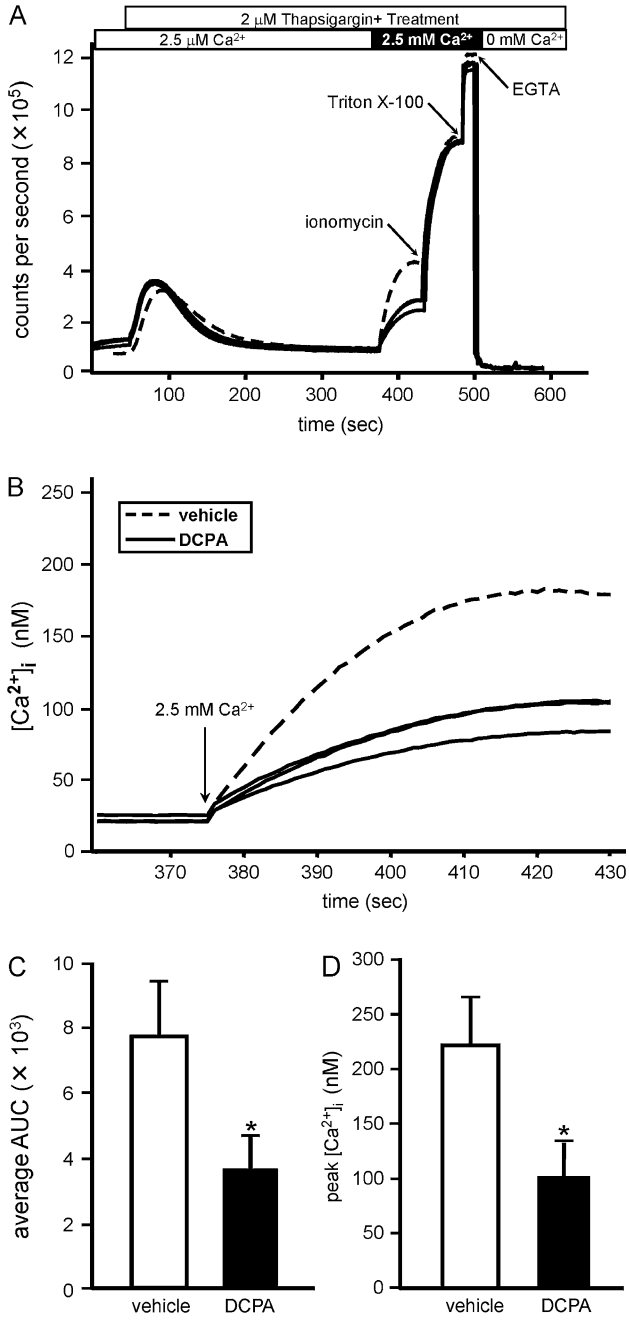

FIG. 2. DCPA does not affect early IP_3-mediated signaling or depletion of ER Ca^{2+} stores. Jurkat cells were loaded with fluo-3 in a nominally Ca^{2+}-free solution. At 50 s, thapsigargin was added simultaneously with 100μM DCPA or vehicle control and changes in $(Ca^{2+})_i$ were recorded with a spectrofluorometer. At 375 s, the external $[Ca^{2+}]$ was raised to 2.5mM with $CaCl_2$. Starting at 430 s, ionomycin, Triton X-100 and EGTA were sequentially added to the cell media at the times indicated. (A) A representative experiment of the complete fluorescence curve of vehicle control (dashed line) and 100μM DCPA-treated cells (solid line). (B) Conversion of the fluorescence intensity from part A to $[Ca^{2+}]_i$ for t = 360–430 s. (C) Statistical analysis of the AUC for DCPA and vehicle control from three separate experiments. (D) Statistical analysis of the peak $[Ca^{2+}]_i$ for DCPA and vehicle control from three separate experiments. Error bars reflect the ± SD and asterisks (*) indicates statistically significant results, $p < 0.05$. Statistical analysis was performed using a t-test.

approximate 55% decrease in the peak $[Ca^{2+}]_i$. This data indicates that early IP_3-induced signaling events and depletion of ER Ca^{2+} stores were not affected by the exposure of Jurkat cells to DCPA. However, the addition of extracellular Ca^{2+} following store depletion resulted in an overall decrease in the available free cytosolic Ca^{2+}.

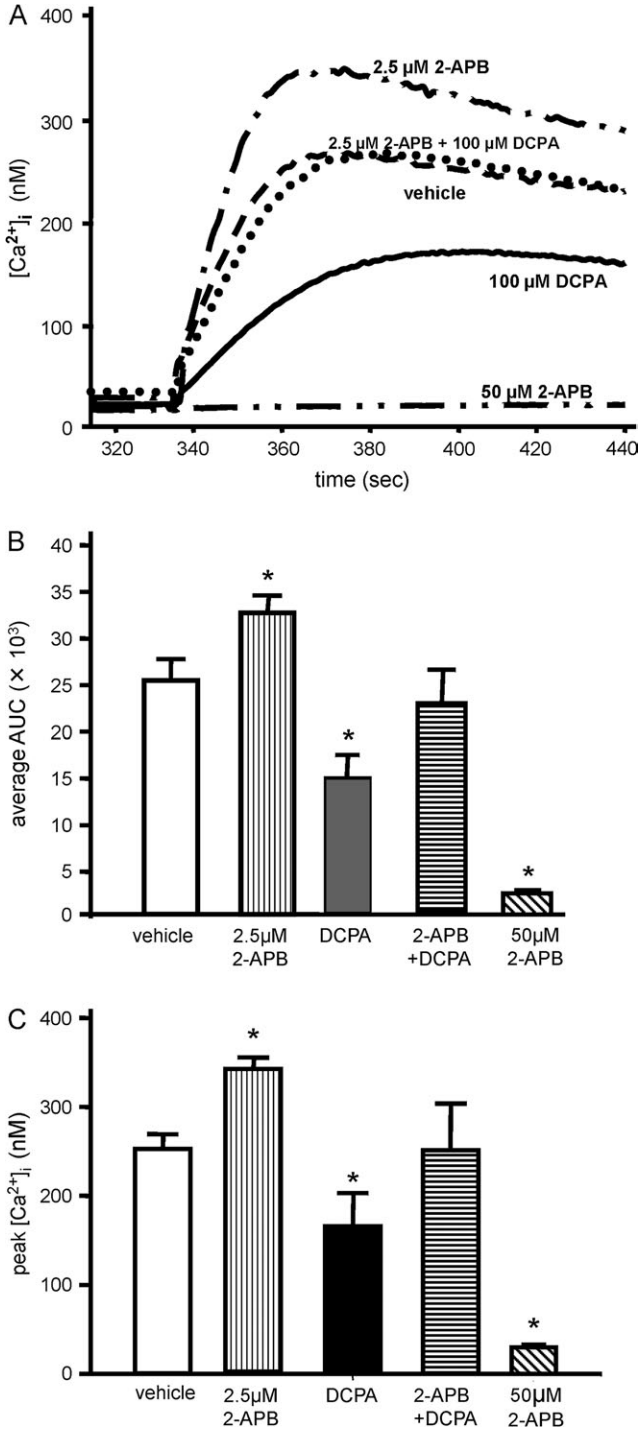

The Effect of DCPA and 2-APB on $[Ca^{2+}]_i$

To further characterize the effect of DCPA on $[Ca^{2+}]_i$, we compared DCPA-induced inhibition with that seen with 2-APB, a known inhibitor and enhancer of Ca^{2+} influx through CRAC channels (Prakriya and Lewis, 2001). At low concentrations (< 5μM) 2-APB enhances Ca^{2+} influx through CRAC channels but at higher concentrations (> 10μM) it inhibits Ca^{2+} influx (Prakriya and Lewis, 2001). Because 2-APB has been shown to alter Ca^{2+} influx following store depletion we compared the effects of 2-APB on $[Ca^{2+}]_i$ to that of DCPA.

Jurkat cells were stimulated with anti-CD3 and the change in $[Ca^{2+}]_i$ was measured in cells treated with vehicle control, 100μM DCPA, 2.5μM 2-APB, 50μM 2-APB, or a mixture of 100μM DCPA and 2.5μM 2-APB (Fig. 3A). As expected there was no change in the release of Ca^{2+} from internal stores regardless of treatment, except for the cells exposed to 50μM 2-APB (data not shown). High concentrations of 2-APB have been reported to affect IP_3-mediated signaling in addition to inhibiting Ca^{2+} influx but IP_3 signaling is not affected at lower enhancing concentrations of 2-APB (Prakriya and Lewis, 2001). Figure 3A shows the changes in $[Ca^{2+}]_i$ following store depletion and the subsequent addition of external Ca^{2+}. Cells treated with 2.5μM 2-APB demonstrated a significant increase in $[Ca^{2+}]_i$ compared with the vehicle control whereas 50μM 2-APB abrogates the increase in the $[Ca^{2+}]_i$ (Fig. 3A). When cells were simultaneously treated with 100μM DCPA and 2.5μM 2-APB the enhanced effect of 2-APB was abrogated.

Cells treated with DCPA or 50μM 2-APB revealed significant decreases in the AUC and the peak $[Ca^{2+}]_i$, as compared with the vehicle control (Figs. 3B and 3C). The AUC and peak $[Ca^{2+}]_i$ were significantly increased (30%) in cells treated with 2.5μM 2-APB (Figs. 3B and 3C). Cells treated simultaneously with 100μM DCPA and 2.5μM 2-APB exhibited a 30% decrease in the AUC and peak $[Ca^{2+}]_i$ when compared with the enhanced influx of 2.5μM 2-APB (Figs. 3B and 3C). Together these results provide further evidence that, following SOC depletion, DCPA-exposed cells decrease $[Ca^{2+}]_i$ in a similar manner as 2-APB and DCPA interferes with the ability of 2-APB to enhance Ca^{2+} influx through CRAC channels.

FIG. 3. The effect of DCPA and 2-APB on $[Ca^{2+}]_i$. Jurkat cells were loaded with fluo-3 in a nominally free Ca^{2+}solution. Anti-CD3 was added simultaneously with 100μM DCPA, 2.5μM 2-APB, 50μM 2-APB, a mixture of 100μM DCPA, and 2.5μM or vehicle control. Fluorescence changes in $(Ca^{2+})_i$ was recorded with a spectrofluorometer and converted to a $[Ca^{2+}]_i$. (A) A representative experiment of the conversion of the fluorescence intensity to a $[Ca^{2+}]_i$ from $t = 300$ to 420 s for DCPA and vehicle control. (B) Statistical analysis of the AUC for DCPA, 2-APB (2.5 and 50μM), 100μM DCPA plus 2.5μM 2-APB and vehicle control from three separate experiments. (C) Statistical analysis of the peak $[Ca^{2+}]_i$ for DCPA, 2-APB (2.5 and 50μM), 100μM DCPA plus 2.5μM 2-APB, and vehicle control from three separate experiments. Error bars reflect the ± SD and asterisks (*) indicates statistically significant change compared with vehicle control, $p < 0.05$. Statistical analysis was performed using a *t*-test.

The Effect of DCPA on Membrane Potential

It is well known that changes in the membrane potential of T cells can alter Ca^{2+} influx (Sarkadi *et al*., 1990). To determine if the effect on $[Ca^{2+}]_i$ seen in DCPA-exposed cells was due to alterations in the membrane potential Jurkat cells were loaded with the membrane potential-sensitive dye, $DiBAC_4(3)$. As the cell depolarizes increasing amounts of the $DiBAC_4(3)$ dye enters the cell membrane resulting in an increased fluorescence signal whereas a decrease in the fluorescence signal indicates hyperpolarization. Jurkat cells were exposed to 100μM DCPA or vehicle control and stimulated with anti-CD3 in a nominally Ca^{2+}-free buffer. Changes in the fluorescence signal using flow cytometry are depicted in Figure 4. The background resting T-cell fluorescence was recorded at $t = 0$. Fluorescence measurements were taken immediately following the simultaneous addition of the treatment and anti-CD3 ($t = 1$ min), then again at $t = 3$ min and $t = 5$ min. External Ca^{2+} was then added and fluorescence measurements were taken immediately at $t =$ 5.5 m, $t = 6.5$, and $t = 9.5$ m. Addition of 50mM KCl at $t = 10$ min depolarized the cell and demonstrated that the dye responds to this depolarization. Further fluorescence measurements were also taken at $t = 12$ and 14 min. This data demonstrates that the DCPA-induced attenuation of $[Ca^{2+}]_i$ following store depletion is not due to changes in the membrane potential.

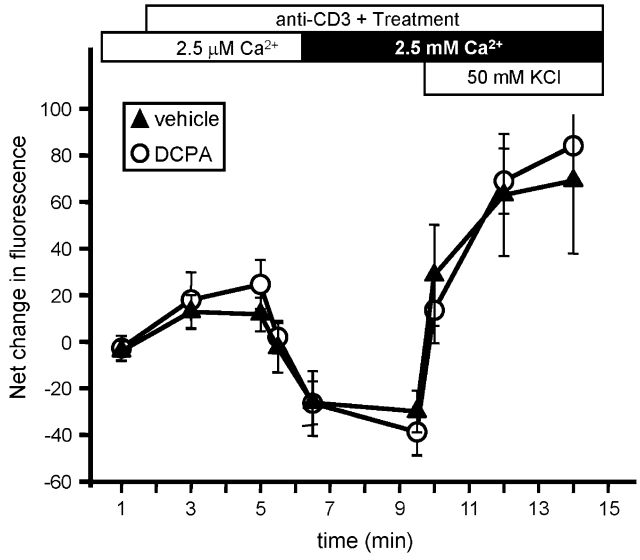

FIG. 4. DCPA does not alter the membrane potential of anti-CD3 stimulated Jurkat cells. Jurkat cells were loaded with $DiBAC_4(3)$ in a nominally Ca^{2+} free solution and analyzed via flow cytometry. Open circles are DCPA-treated cells and closed triangles are vehicle control cells. At $t = 0$ the background resting potential was recorded. Fluorescence measurements were taken immediately following addition of anti-CD3 and treatment ($t = 1$ min), then again at $t = 3$ min and $t = 5$ min. External Ca^{2+} (2.5mM $CaCl_2$) was then added and fluorescence measurements were recorded at $t = 5.5$ min, $t = 6.5$, and $t = 9.5$ min. Fifty millimolar KCl was added to depolarize the cells and fluorescence measurements were taken at $t = 10$, 12, and 14 min. Error bars reflect the ± SD from three experiments. Statistical analysis was performed using a *t*-test.

Effect of DCPA on IL-2 Secretion in Jurkat Cells

A reduction in the elevated $[Ca^{2+}]_i$ following store depletion has direct downstream affects on Ca^{2+}-dependent pathways. In order to establish a functional consequence of exposure to DCPA we assessed its effect on IL-2 secretion. IL-2 is an essential early cytokine required for T-cell proliferation and differentiation. The activation of transcription factors NF-κB, NFAT, and AP-1, depend, to varying degrees, on the $[Ca^{2+}]_i$ and are important in the production of IL-2. Jurkat cells were stimulated with anti-CD3 and anti-CD28 and exposed to 25, 50, 100, or 200μM DCPA or vehicle control. In order to obtain optimal IL-2 production Jurkat cells require costimulation with both anti-CD3 and anti-CD28. After 48 h in culture, IL-2 levels in the supernatant were assayed via a sandwich ELISA. The results of a representative experiment are shown in Table 1. In the presence of 2.5mM extracellular Ca^{2+}, DCPA decreased IL-2 production in a concentration-dependent manner, with no detectable IL-2 production when exposed to 200μM DCPA. Exposure of Jurkat cells to 100μM DCPA inhibited IL-2 production by 72%. In experiments performed with the same DCPA and vehicle control concentrations but with nominal extracellular Ca^{2+} ($\leq$ 2.5μM), no detectable levels of IL-2 were measured (data not shown).

Effect of DCPA on Nuclear Translocation of NFAT

In order to establish a direct mechanistic consequence of DCPA on the inhibition of Ca^{2+}-dependent signaling events we examined the Ca^{2+}-dependent transcription factor NFAT. A sustained $[Ca^{2+}]_i$ via Ca^{2+} influx results in the calmodulin-stimulated activation of the protein phosphatase, calcineurin (Lewis, 2001; Feske *et al*., 2003; Quintana *et al*., 2005). Calcineurin dephosphorylates cytoplasmic NFAT allowing its translocation into the nucleus where is acts as a transcription factor for many genes, including IL-2. To assess the effect of DCPA on NFAT we measured the levels of nuclear NFAT at various time points after T-cell stimulation. Jurkat cells were treated with vehicle control, 100μM DCPA or no treatment and stimulated with PMA and A23187. After 1, 2, 4, or 6 h

TABLE 1
Effects of DCPA on IL-2 Production

Treatment	IL-2	% Control
No treatment	3420 ± 272	97.4
Vehicle control	3510 ± 564	100.0
25μM DCPA	2720 ± 169	77.5
50μM DCPA	2262 ± 312	64.4
100μM DCPA	968 ± 245	27.6
125μM DCPA	1171 ± 137	33.4
200μM DCPA	< 32[a]	

Note. IL-2 is measured in μg/ml ± SD.
[a]Below the level of detection.

incubations nuclear extracts were made and the level of nuclear NFAT was determined by western blot. Cells exposed to 100μM DCPA exhibited decreases in nuclear NFAT at all time points (Figs. 5A and 5B). Densitometric analysis of the decrease in nuclear NFAT in DCPA-treated Jurkat cells indicated that 100μM DCPA decreased nuclear NFAT approximately 30% compared with the vehicle control (Fig. 5C). Because NFAT is a Ca^{2+}-dependent transcription factor, this data demonstrates a direct mechanism linking the decrease in $[Ca^{2+}]_i$ observed in DCPA-treated cells to decreased IL-2 production.

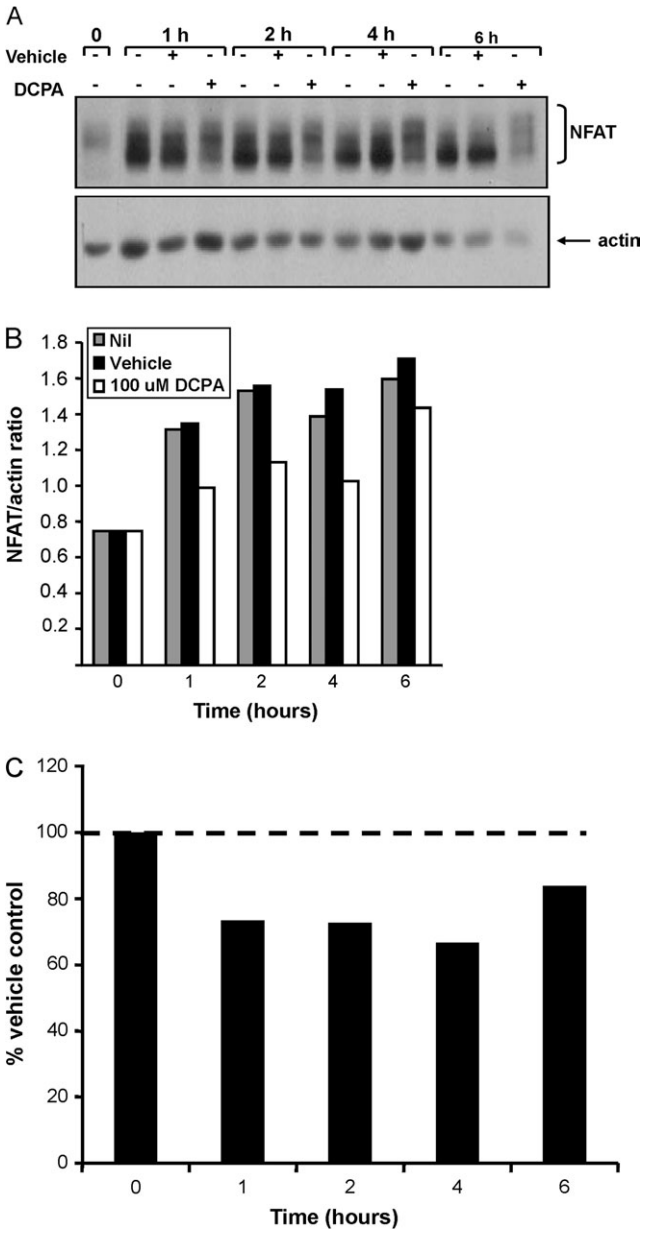

FIG. 5. DCPA decreases nuclear NFAT levels. Nuclear extracts from Jurkat cells were stimulated and exposed to 100μM DCPA at various time points. (A) A representative blot indicating the bands that represent different forms of NFAT (top blot). The bands in the bottom blot are β-actin levels used as a loading and transfer control. (B) The ratio of NFAT protein to β-actin protein using densitometry of the bands in (A). (C) The percent of control based on the differences between the NFAT:β-actin ratio of the vehicle and the DCPA treated samples at the indicated time points. Dotted line represents 100% of the control at each time point.

Effect of DCPA on Primary Mouse T Cells

In order to establish that the DCPA-induced attenuation of $[Ca^{2+}]_i$ was not unique to the Jurkat cell line, we assayed the effect of DCPA on $[Ca^{2+}]_i$ levels in primary mouse T cells. Splenic T cells were isolated from female BALB/c mice by

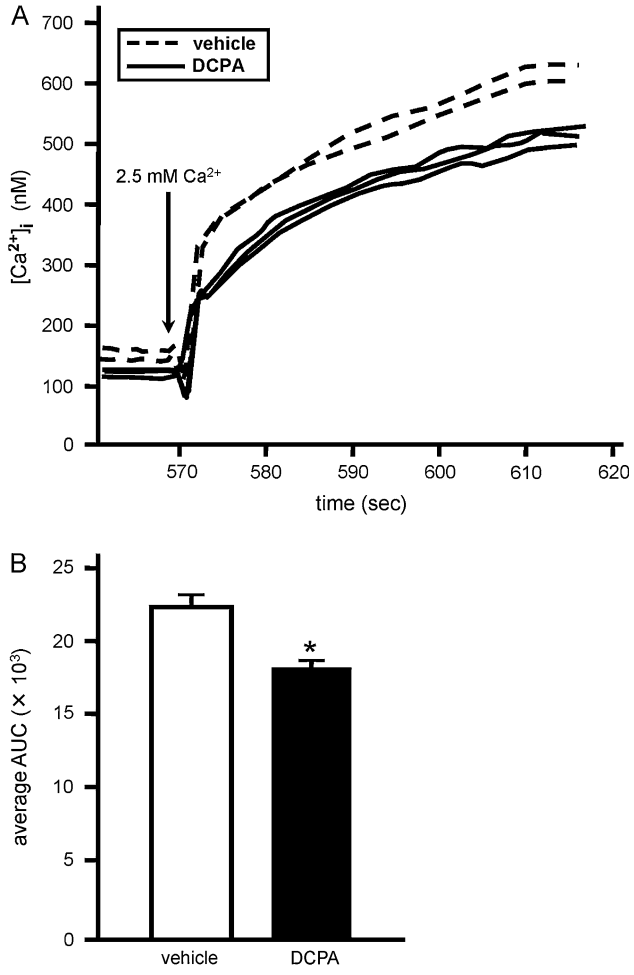

FIG. 6. The effect of DCPA on $[Ca^{2+}]_i$ in primary mouse T cells. Purified mouse splenic T cells were loaded with fluo-3 in a nominally Ca^{2+}-free solution. Anti-CD3 was added simultaneously with 100μM DCPA or vehicle control and changes in Ca^{2+} fluorescence was recorded with a spectrofluorometer. At 567 s, the external $[Ca^{2+}]$ was raised to 2.5mM with $CaCl_2$. Starting at 620 s, ionomycin, Triton X-100 and EGTA were sequentially added to the cell media at the times indicated. (A) A representative experiment showing the $[Ca^{2+}]_i$ for 560–620 s in the presence of vehicle control (solid line) or 100μM DCPA (dashed line). (B) Statistical analysis of the AUC for DCPA and vehicle control. Error bars reflect the ± SD from two experiments and analysis was performed using a student *t*-test, $p < 0.05$.

negative selection and magnetic sorting. The T cells were loaded with fluo-3 and the effect of 100μM DCPA on $[Ca^{2+}]_i$ was assayed as described previously. DCPA exposure did not affect the anti-CD3 induced release of Ca^{2+} from internal stores (data not shown). However, there was a significant decrease in $[Ca^{2+}]_i$ following store depletion and addition of external Ca^{2+} (Fig. 6). There were not enough data points to assess the change in peak $[Ca^{2+}]_i$ but the AUC ($t = 517–616$ s) was significantly decreased (16%) in the DCPA-treated cells (Fig. 6B). Altogether, these results demonstrate that the effect of DCPA on Ca^{2+} influx following store depletion is not limited to the human Jurkat T cells.

DISCUSSION

DCPA is a widely used herbicide that is heavily applied on rice crops. Its recent registration for use on turf may further increase not only its application but the likelihood of human exposure to DCPA (Edwards, 2006). The U.S. Environmental Protection Agency conducted an exposure risk assessment for workers involved in mixing, loading and applying DCPA (Edwards, 2006). The results from this assessment indicate that workers using maximal protection, including closed mixing and loading systems and enclosed cockpit, cabs or trucks, are at risk for exposure to DCPA (Edwards, 2006). Workers entering treated areas 12 h after application were also at risk being exposed to levels above stated limits (Edwards, 2006). In determining risk levels, the EPA considers workers at risk if they have a margin of exposure (MOE) value less than 300. This value is used to determine how close a worker comes to the no observed adverse effects level (NOAEL). Workers entering treated areas 12 hours after application had MOE values as low as 4 and were therefore considered at risk to exposure to DCPA(EPA 2006). In addition, there have also been reports of nonoccupational exposure, including a child under the age of 6 (Edwards, 2006). These conclusions emphasize the need to investigate the effects of human exposure to DCPA.

The effects of DCPA in the rodent model have been well established. In a mouse model, exposure to DCPA results in thymic atrophy, depressed Natural Killer cell (NK) and macrophage functions, altered cytotoxic T-cell response, and decreased $CD4^+$ T cells (Barnett and Gandy, 1989; Sheil *et al.*, 2006; Ustyugova *et al.*, 2007; Zhao *et al.*, 1995). The number of reports on the effect of DCPA on human immune cells is limited. Human macrophages exposed to DCPA produce reduced levels of TNF-α, reactive oxygen species and reactive nitrogen species (Ustyugova *et al.*, 2007). Human T cells exposed to DCPA exhibit decreased IL-2 production and decreased binding of transcription factor AP-1 to DNA (Brundage *et al.*, 2004). Although DCPA does not disrupt the overall lipid bilayer fluidity in stimulated Jurkat cells there is a small spectral component (less mobile) observed by electron spin resonance spectroscopy. These data suggest that DCPA increased the number of probes in the restricted motional environment following cell stimulation without affecting the motional properties of the particular lipids (Brundage *et al.*, 2003). Finally, Corsini *et al.* (2007) examined agricultural workers exposed to DCPA and reported alterations in leukocyte cytokine production.

Because the sustained and elevated influx of Ca^{2+}, following store depletion, is necessary for T-cell activation and proliferation, we examined the effects of DCPA on $[Ca^{2+}]_i$. Our experiments using Jurkat and mouse splenic T cells demonstrate that DCPA attenuates the increased $[Ca^{2+}]_i$ following store depletion in a concentration dependent manner. Anti-CD3 or thapsigargin induced store depletion in DCPA-exposed Jurkat cells did not affect IP_3-mediated release of Ca^{2+} nor the depletion of ER Ca^{2+} stores. The reduced nuclear NFAT levels and IL-2 production is likely a consequence of this attenuation.

2-APB is widely used as both an inhibitor and enhancer of Ca^{2+} influx through CRAC channels (Prakriya and Lewis, 2001, 2006). Low concentrations of 2-APB ($\leq$ 5.0μM) enhances Ca^{2+} influx through CRAC channels following store depletion but do not affect IP_3-mediated release of Ca^{2+} from the ER (Prakriya and Lewis, 2001). High concentrations of 2-APB ($\geq$ 50μM) block Ca^{2+} influx through CRAC channels (Prakriya and Lewis, 2001). We used 2-APB to further investigate the inhibitory role of DCPA in Ca^{2+} signaling. Jurkat cells exposed to a mixture of 100μM DCPA and 2.5μM 2-APB abrogated the enhanced Ca^{2+} influx seen with 2.5μM 2-APB. This data suggests that T cells exposed to DCPA prevent the increased influx of Ca^{2+} seen at low concentrations of 2-APB by inhibiting events surrounding CRAC channel activation.

Both voltage-gated and Ca^{2+}-activated potassium (K^+) channels are PM channels involved in regulating the polarization state of T cells and modulating the rate of Ca^{2+} influx through CRAC channels (Lewis, 2001; Panyi *et al.*, 2004; Quintana *et al.*, 2005). Alterations in K^+ channels can change the polarization state and impact Ca^{2+} influx (Panyi *et al.*, 2004). Depolarization of the cell can inhibit Ca^{2+} influx whereas hyperpolarization increases the driving for force of Ca^{2+} into the cell. Our experiments indicate that DCPA does not alter the membrane potential of T cells (Fig. 4) and therefore DCPA is unlikely to affect these channels.

In T cells, the plasma membrane Ca^{2+}-ATPase (PMCA) pump is considered the primary Ca^{2+} extrusion mechanism. Modulation of PMCA activity can occur in response to an influx of Ca^{2+} through CRAC channels and results in long term stability of the Ca^{2+} signal (Feske *et al.*, 2005). Because we have demonstrated that DCPA-treated cells attenuate the increase in $[Ca^{2+}]_i$ following store depletion it may be possible that DCPA enhances PMCA activity and thereby reduces the apparent amount of cytosolic Ca^{2+}. However, this mechanism appears unlikely because PMCA activity could also result in

a decrease $[Ca^{2+}]_i$ during the initial IP_3-mediated release of Ca^{2+} from internal stores. Figures 1A, 2A, and 3A demonstrate no change in $[Ca^{2+}]_i$ during the initial IP_3-mediated release of Ca^{2+} from internal stores in DCPA-treated cells. However, without direct evidence of the target(s) for DCPA, this mechanism cannot be definitively ruled out.

The mitochondria also play an important role in Ca^{2+} homeostasis (Parekh, 2003; Quintana *et al*., 2005). Mitochondria can act as a Ca^{2+} sink and sequester large amounts of Ca^{2+} quickly and release it slowly after Ca^{2+} influx subsides (Parekh, 2003). Expression of a uniporter in the mitochondrial inner membrane and a Na^+/Ca^{2+} exchanger allow for Ca^{2+} uptake and release, respectively (Parekh, 2003). Alterations in the activity of the uniporter, Na^+/Ca^{2+} exchanger or altered membrane potential of the mitochondrial membrane could result in an apparent decrease in Ca^{2+} influx. Any increased function of Ca^{2+} uptake by the mitochondria would also result in an apparent decrease the initial IP_3-mediated release of Ca^{2+} from internal stores, which was not observed in DCPA-exposed T cells. However, because we have not investigated the effects of DCPA directly on the mitochondria function, this mechanism is still possible.

Our data indicates that DCPA alters Ca^{2+} homeostasis in human and murine T cells. Specifically, DCPA is able to attenuate the increase in $[Ca^{2+}]_i$ following store depletion. The ability of DCPA to abrogate the enhanced Ca^{2+} influx produced by 2.5μM 2-APB through CRAC channels provides some evidence that DCPA is acting on mechanisms involved in the activation or regulation of CRAC channels. This decrease in $[Ca^{2+}]_i$ has significant downstream consequences on nuclear NFAT levels and secretion of IL-2. From the studies reported herein, it is clear that the decrease in $[Ca^{2+}]_i$ results in a functional consequence to human T cells. The data also demonstrates that exposure to DCPA alters $[Ca^{2+}]_i$ in murine and human Jurkat T cells which may result in immunosuppression with serious consequences on human health.

FUNDING

National Institutes of Health grants (ES11311 and ES010953) to J.B.B., and (RR016440) for flow cytometry; Environmental Protection Agency Greater Research Opportunity Fellowship (MA-91684801-0) to T.L.L.

ACKNOWLEDGMENTS

We would like to thank Dr William Atchison for his helpful advice on this project and Dr Cynthia Cunningham for her help in the flow cytometry facility.

The findings and conclusions in this report are those of the authors and do not necessarily represent the views of the National Institute for Occupational Safety and Health.

REFERENCES

Abraham, R. T., and Weiss, A. (2004). Jurkat T cells and development of the T-cell receptor signalling paradigm. *Nat. Rev. Immunol.* **4,** 301–308.

Barnett, J. B., and Gandy, J. (1989). Effect of acute propanil exposure on the immune response of C57Bl/6 mice. *Fundam. Appl. Toxicol.* **12,** 757–764.

Barnett, J., Gandy, J., Wilbourn, D., and Theus, S. A. (1992). Comparison of the immunotoxicity of propanil and its metabolite, 3,4-dichloroaniline, in C57Bl/6 mice. *Fundam. Appl. Toxicol.* **18,** 626–631.

Bergling, S., Dolmetsch, R., Lewis, R. S., and Keizer, J. (1998). A fluorometric method for estimating the calcium content of internal stores. *Cell Calcium* **23,** 251–259.

Brundage, K. M., Barnett, J. B., and Mahaney, J. E. (2003). The amide class herbicide 3,4-dichloropropionanilide (DCPA) alters the mobility of hydrocarbon chains in T-lymphocyte but not macrophage membranes. *J. Toxicol. Environ. Health A* **66,** 2253–2265.

Brundage, K. M., Schafer, R., and Barnett, J. B. (2004). Altered AP-1 (activating protein-1) activity and c-jun activation in T cells exposed to the amide class herbicide 3,4-dichloropropionanilide (DCPA). *Toxicol. Sci.* **79,** 98–105.

Corsini, E., Codeca, I., Mangiaratti, S., Birindelli, S., Minoia, C., Turci, R., Viviani, B., Facchi, A., Vitelli, N., Lucchi, L., *et al*. (2007). Immunomodulatory effects of the herbicide propanil on cytokine production in humans: In vivo and in vitro exposure. *Toxicol. Appl. Pharmacol.* **222,** 202–210.

Edwards, D. (2006). Amendment to Reregistration Eligibility Decision (RED) for Propanil (March 2006) and the Propanil RED (September 2003). United States Environmental Protection Agency. Available at http://www.epa.gov/oppsrrd1/REDs/propanil_red_combined.pdf.

Feske, S. (2007). Calcium signalling in lymphocyte activation and disease. *Nat. Rev. Immunol.* **7,** 690–702.

Feske, S., Draeger, R., Peter, H. H., and Rao, A. (2000). Impaired NFAT regulation and its role in a severe combined immunodeficiency. *Immunobiology* **202,** 134–150.

Feske, S., Giltnane, J., Dolmetsch, R., Staudt, L. M., and Rao, A. (2001). Gene regulation mediated by calcium signals in T lymphocytes. *Nat. Immunol.* **2,** 316–324.

Feske, S., Gwack, Y., Prakriya, M., Srikanth, S., Puppel, S. H., Tanasa, B., Hogan, P. G., Lewis, R. S., Daly, M., and Rao, A. (2006). A mutation in Orai1 causes immune deficiency by abrogating CRAC channel function. *Nature* **441,** 179–185.

Feske, S., Okamura, H., Hogan, P. G., and Rao, A. (2003). Ca2+/calcineurin signalling in cells of the immune system. *Biochem. Biophys. Res. Commun.* **311,** 1117–1132.

Feske, S., Prakriya, M., Rao, A., and Lewis, R. S. (2005). A severe defect in CRAC Ca2+ channel activation and altered K+ channel gating in T cells from immunodeficient patients. *J. Exp. Med.* **202,** 651–662.

Garrity, P. A., Chen, D., Rothenberg, E. V., and Wold, B. J. (1994). Interleukin-2 transcription is regulated in vivo at the level of coordinated binding of both constitutive and regulated factors. *Mol. Cell Biol.* **14,** 2159–2169.

Grynkiewicz, G., Poenie, M., and Tsien, R. Y. (1985). A new generation of Ca2+ indicators with greatly improved fluorescence properties. *J. Biol. Chem.* **260,** 3440–3450.

Kubo, R. T., Born, W., Kappler, J. W., Marrack, P., and Pigeon, M. (1989). Characterization of a monoclonal antibody which detects all murine alpha beta T cell receptors. *J. Immunol.* **142,** 2736–2742.

Lewis, R. S. (2001). Calcium signaling mechanisms in T lymphocytes. *Annu. Rev. Immunol.* **19,** 497–521.

Panyi, G., Varga, Z., and Gaspar, R. (2004). Ion channels and lymphocyte activation. *Immunol. Lett.* **92,** 55–66.

Parekh, A. B. (2003). Store-operated Ca2+ entry: Dynamic interplay between endoplasmic reticulum, mitochondria and plasma membrane. *J. Physiol.* **547,** 333–348.

Prakriya, M., Feske, S., Gwack, Y., Srikanth, S., Rao, A., and Hogan, P. G. (2006). Orai1 is an essential pore subunit of the CRAC channel. *Nature* **443,** 230–233.

Prakriya, M., and Lewis, R. S. (2001). Potentiation and inhibition of Ca(2+) release-activated Ca(2+) channels by 2-aminoethyldiphenyl borate (2-APB) occurs independently of IP(3) receptors. *J. Physiol.* **536,** 3–19.

Prakriya, M., and Lewis, R. S. (2006). Regulation of CRAC channel activity by recruitment of silent channels to a high open-probability gating mode. *J. Gen. Physiol.* **128,** 373–386.

Quintana, A., Griesemer, D., Schwarz, E. C., and Hoth, M. (2005). Calcium-dependent activation of T-lymphocytes. *Pflugers Arch.* **450,** 1–12.

Sarkadi, B., Tordai, A., and Gardos, G. (1990). Membrane depolarization selectively inhibits receptor-operated calcium channels in human T (Jurkat) lymphoblasts. *Biochim. Biophys. Acta* **1027,** 130–140.

Schreiber, E., Matthias, P., Muller, M. M., and Schaffner, W. (1989). Rapid detection of octamer binding proteins with 'mini-extracts', prepared from a small number of cells. *Nucleic Acids Res.* **17,** 6419.

Sheil, J. M., Frankenberry, M. A., Schell, T. D., Brundage, K. M., and Barnett, J. B. (2006). Propanil exposure induces delayed but sustained abrogation of cell-mediated immunity through direct interference with cytotoxic T-lymphocyte effectors. *Environ. Health Perspect.* **114,** 1059–1064.

Ustyugova, I. V., Frost, L. L., Van Dyke, K., Brundage, K. M., Schafer, R., and Barnett, J. B. (2007). 3,4-dichloropropionaniline suppresses normal macrophage function. *Toxicol. Sci.* **97,** 364–374.

Vig, M., Peinelt, C., Beck, A., Koomoa, D. L., Rabah, D., Koblan-Huberson, M., Kraft, S., Turner, H., Fleig, A., Penner, R., *et al.* (2006). CRACM1 is a plasma membrane protein essential for store-operated Ca2+ entry. *Science* **312,** 1220–1223.

Wolff, C., Fuks, B., and Chatelain, P. (2003). Comparative study of membrane potential-sensitive fluorescent probes and their use in ion channel screening assays. *J. Biomol. Screen.* **8,** 533–543.

Wu, M. M., Buchanan, J., Luik, R. M., and Lewis, R. S. (2006). Ca2+ store depletion causes STIM1 to accumulate in ER regions closely associated with the plasma membrane. *J. Cell Biol.* **174,** 803–813.

Xie, Y. C., Schafer, R., and Barnett, J. B. (1997). Inhibitory effect of 3,4-dichloro-propionaniline on cytokine production by macrophages is associated with LPS-mediated signal transduction. *J. Leukoc. Biol.* **61,** 745–752.

Xu, P., Lu, J., Li, Z., Yu, X., Chen, L., and Xu, T. (2006). Aggregation of STIM1 underneath the plasma membrane induces clustering of Orai1. *Biochem. Biophys. Res. Commun.* **350,** 969–976.

Zhang, S. L., Yu, Y., Roos, J., Kozak, J. A., Deerinck, T. J., Ellisman, M. H., Stauderman, K. A., and Cahalan, M. D. (2005). STIM1 is a Ca2+ sensor that activates CRAC channels and migrates from the Ca2+ store to the plasma membrane. *Nature* **437,** 902–905.

Zhao, W., Schafer, R., and Barnett, J. B. (1998). Cytokine production by C57BL/6 mouse spleen cells is selectively reduced by exposure to propanil. *J. Toxicol. Environ. Health A* **55,** 107–120.

Zhao, W., Schafer, R., and Barnett, J. B. (1999). Propanil affects transcriptional and posttranscriptional regulation of IL-2 expression in activated EL-4 cells. *Toxicol. Appl. Pharmacol.* **154,** 153–159.

Zhao, W., Schafer, R., Cuff, C. F., Gandy, J., and Barnett, J. B. (1995). Changes in primary and secondary lymphoid organ T-cell subpopulations resulting from acute in vivo exposure to propanil. *J. Toxicol. Environ. Health* **46,** 171–181.